

Article

# Modified U-shaped Microactuator with Compliant Mechanism Applied to a Microgripper

Pedro Vargas-Chable <sup>1</sup>, Margarita Tecpoyotl-Torres <sup>1,\*</sup> , Ramon Cabello-Ruiz <sup>2</sup>,  
Jose Alfredo Rodriguez-Ramirez <sup>1</sup>  and Rafael Vargas-Bernal <sup>3</sup> 

<sup>1</sup> Instituto de Investigación en Ciencias Básicas y Aplicadas-Centro de Investigación en Ingeniería y Ciencias Aplicadas (IICBA-CIICAp), Universidad Autónoma del Estado de Morelos (UAEM), Cuernavaca 62209, Mor., Mexico; pedro.vargas@uaem.mx (P.V.-C.); jarr@uaem.mx (J.A.R.-R.)

<sup>2</sup> Universidad Tecnológica Emiliano Zapata, Emiliano Zapata 62765, Mor., Mexico; ramon.cabello@uaem.mx

<sup>3</sup> Departamento de Ingeniería en Materiales, Instituto Tecnológico Superior de Irapuato (ITESI). Carretera Irapuato-Silao Km 12.5, Col. El Copal. Irapuato 36821, Gto., Mexico; ravargas@itesi.edu.mx

\* Correspondence: tecpoyotl@uaem.mx

Received: 17 January 2019; Accepted: 15 March 2019; Published: 19 March 2019



**Abstract:** In this paper, a modified U-shaped micro-actuator with a compliant mechanism is proposed. It was analyzed with a uniform and modified thin arm, as well as a similar variation in the corresponding flexure, in order to observe the impact of the compliant lumped mechanism. The use of these compliant mechanisms implies an increment in the deformation and a reduction in the equivalent stress of 25% and 52.25%, respectively. This characterization was developed using the Finite Element Method (FEM) in ANSYS Workbench. The design, analysis and simulation were developed with Polysilicon. In this study, the following performance parameters were also analyzed: force and temperature distribution. This device is supplied with voltage from 0 V up to 3 V, at room temperature. The modified U-shaped actuator was applied in both arms of a microgripper, and to evaluate its electrothermal performance, a static structural analysis has been carried out in Ansys Workbench. The microgripper has an increment in deformation of 22.33%, an equivalent stress reduction of 50%, and a decrease in operation frequency of 10.8%. The force between its jaws is of 367  $\mu$ N. This low level of force could be useful when sensitive particles are manipulated.

**Keywords:** Polysilicon; electrothermal actuation; dimples; ANSYS

## 1. Introduction

The U-shaped actuator is a typical microelectromechanical (MEM) device, which has been used to design and construct several microgrippers reported in the literature. This basically consists of two joined line-shaped beams, where one of them is thin (hot arm), and the other one is wide (cold arm). They are restricted by two anchors [1]. A smaller beam, called flexure, is found between the wide beam and its corresponding anchor. The U-shaped actuator operation is based on the differential thermal expansion between a pair of arms of different widths [2]. When the electrical current flows, the higher electrical current density due to the reduced dimensions of the actuator, causes a dissipation of heat, and the thermal expansion of the hot arm reduces the gap between both arms, through the transverse movement that is produced by a mechanical arching action of the hot arm towards the cold arm.

A microgripper can be defined as a microscopic device used to manipulate microscale objects safely [1]. The microgrippers or micro-tweezers have opened the opportunity to develop manipulation and transport of micro-objects with high precision and reliability in applications such as micro-assembly, micro-robotics, biology, medicine and micro-optics [3–6]. According to their working principle, the actuators for MEM microgrippers can be classified into [1]: electrostatic [7],

electromagnetic [8,9], electrothermal [10], electrochemical [11] and piezoelectric [12], and operated using a shape memory alloy [13]. A review of the state of the art of microgrippers based on microelectromechanical systems (MEMS) is found in [13]. According to the principle of the microgripper, a wide variety of materials has been used for its manufacture. For example, the processing SOI wafers, shown in [14], allows selected features of a microdevice to be constructed using the thin buried oxide layer, while using the bulk of the silicon wafer creates devices with high-aspect-ratio for sensing and actuation applications. A summary of the state-of-the-art of the advance that has been obtained in the development of microgrippers is given in Table 1.

**Table 1.** State of the art of advances in microgrippers.

Description	Displacement or Opening ( $\mu\text{m}$ )	Force ( $\mu\text{N}$ )	Dimensions ( $\mu\text{m}$ )	Material	Feeding	Ref.
Electrostatic microgripper with capacitive force sensor.	70.88	190	$\sim 6900 \times 6500 \times 500$	Silicon	120 V	[7]
Thermally actuated polymeric microgripper with bare gold working electrode.	50–150	N/A	$1500 \times 100 \times 50$	SU-8/Gold	2 V	[11]
Microgripper with 6 degrees of freedom.	5	N/A	$17000 \times 5000 \times 150$	SU-8/PZT	10 V	[12]
Electrothermal microgripper with chevron micro-actuator.	1.39	N/A	$\sim 102 \times 35 \times 1$	Nickel	28 mA	[15]
Microgripper with chevron micro-actuator rotated at $90^\circ$ .	42	N/A	$\sim 772 \times 350 \times 10$	Silicon	100 mW	[16]
Microgripper for cell manipulation.	37	N/A	$\sim 1000 \times 80 \times 7$	SU-8/Gold	45 V	[17]
Microgrippers driven by a chevron electrothermal actuator.	80	$\sim 200$	$2900 \times 3500 \times 45$	SU-8	53 mV	[18]
Pneumatically operated microgripper.	120	10000	$75000 \times 10,000 \times 360$	SU-8-SMA	400 mbar	[19]
Optimization of the compliant elements of a Microgripper.	40	N/A	$\sim 6000 \times 1000 \times 100$	Polysilicon	3 V	[20]
Microgripper with controlled force.	67	0.0385	N/A	Silicon	10 V	[21]
Electrostatic microgripper with capacitive force sensor.	70	190	$\sim 1125 \times 900 \times 50$	Silicon	120 V	[22]
Microgripper for tissues.	14.2–40.8 30.8–153.4		$2000 \times 2000 \times 80$	Silicon Nickel	1.5–3 V 0.05–0.2 V	[23]
Electrothermal microgripper.	310.6	N/A	$\sim 13500 \times 2500 \times 180$	Silver/Ni-ckel	0.26 A	[24]
Electrostatic microgripper with capacitive sensor.	17	N/A	$5003 \times 6500 \times 25$	Silicon	50 V	[25]
Microgripper design using two in-plane chevron electrothermal actuators, in Polysilicon.	19.2	37000	$\sim 870 \times 200 \times 10$	Polysilicon	0–1.2 V	[26]
Microgripper with rotating element for biomedical applications.	40	N/A	$3860 \times 50 \times 7$	Polysilicon	23.4–129.2 V with freq. of 463.8 Hz	[27]
TiNi film based micro-gripper with compliant structure.	200	N/A	$\sim 4500 \times 200 \times 150$	TiNi	100 $^\circ\text{C}$	[28]

In addition, a survey of microgrippers design can be found in [29], where distinction between lumped and distributed compliance is used in the Atlas preparation.

On the other hand, a compliant mechanism can be defined as a flexible device that transforms the forces or movements of entrance towards another port in a set of forces or movements of exit through the elastic deformation of the body [30]. They can be classified as monolithic (when they are made from a single piece) or jointless structures. Microgrippers are manufactured regularly using compliant mechanisms based on electric actuators.

The modeling of each new device is a necessary task to determine its behavior, before manufacturing it, to achieve an efficient use of it and to know in advance its possible applications. ANSYS is a software used to simulate engineering problems using finite element analysis (FEM). This allows to simulate structures or components of machines to determine mechanical and electrical properties, using the three-dimensional model of the object and the physical properties of the material [31].

This article is focused on a modified U-shaped actuator, which was designed using as reference the one shown in [2]. This micro-actuator is implemented in the initial microgripper given in [2]. Electrothermal actuation is considered in both devices. From initial U-shaped actuator design, thin arm and flexure were modified, considering no uniformly distributed mass. The purpose of this work is to observe the improvement in the U-shaped actuator's performance when these modifications are implemented.

The performance study was done theoretically using a resistive electrical model, and computationally using ANSYS, with Polysilicon as structural material. The main advantage of the modified microgripper, with non-uniform mass distribution, lies in the increment of displacement value (22.33%), but the considerable decrement in force reduces its range of applications to cases when this characteristic would be useful.

The content of this work is organized as follows. Materials and methods are presented in Section 2, where the U-shaped actuators and microgripper designs are provided as well as the theoretical bases for the calculation of some parameters of the microgripper. Analytical calculations and results obtained from simulation for all structures under analysis are given in Section 3. Section 4 discusses the results shown in Section 3. Finally, Section 5 summarizes the findings and provides some concluding remarks.

## 2. Materials and Methods

The initial model is the U-shaped actuator given in [2], (see Figure 1). On the base of it, a modified U-shaped actuator (Figure 2) was developed. Proposed modifications were performed in thin arm and flexure, considering an arrangement of mass distribution. A zoom in of the thin beam is shown in Figure 3, where proportions related to  $L$ , the total length of the modified beam, show the criteria for the length calculation of each segment. In addition, the proportions about the widths are also given.

In all devices under consideration in this work, Polysilicon is used as a structural material with a thickness value of  $1.5 \mu\text{m}$ . It is possible to fabricate all devices presented here using the PolyMUMPS process.

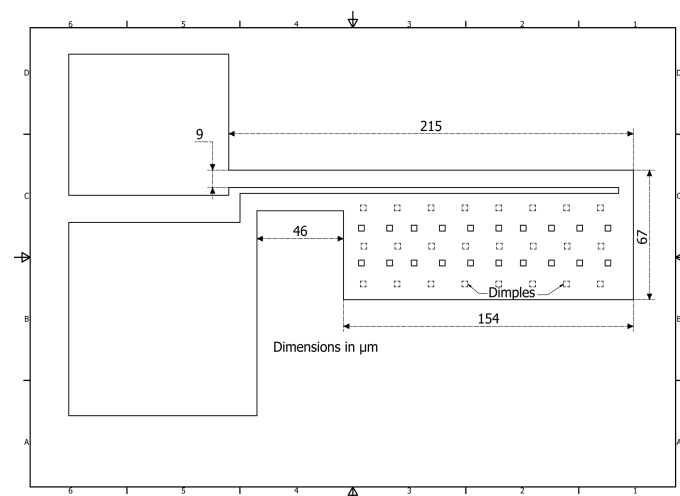


**Figure 1.** Geometry and dimensions of the initial U-shaped micro-actuator, based in [2].

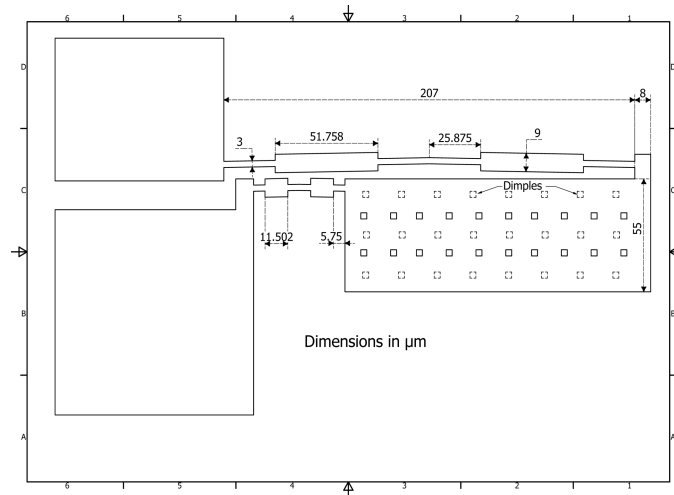


Figure 2. Geometry with dimensions of the proposed modified U-shaped micro-actuator.

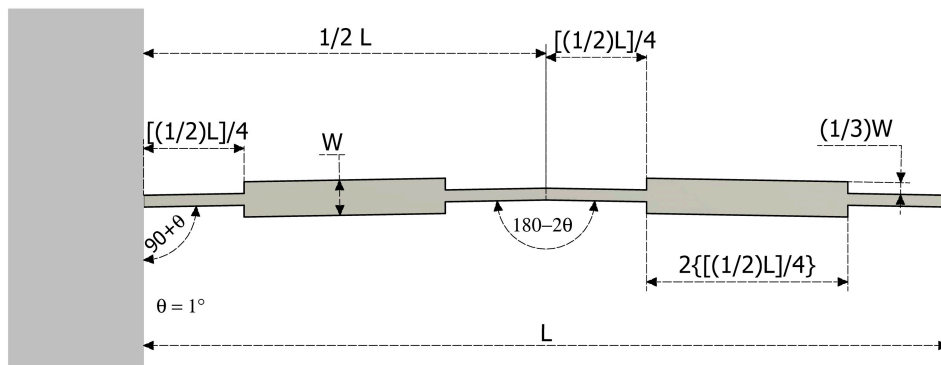


Figure 3. Geometry of the thin beam with distributed mass.

In order to observe the effect of the modified U-shaped actuator, the form of the microgripper is similar to the one presented also in [2] (Figure 4).

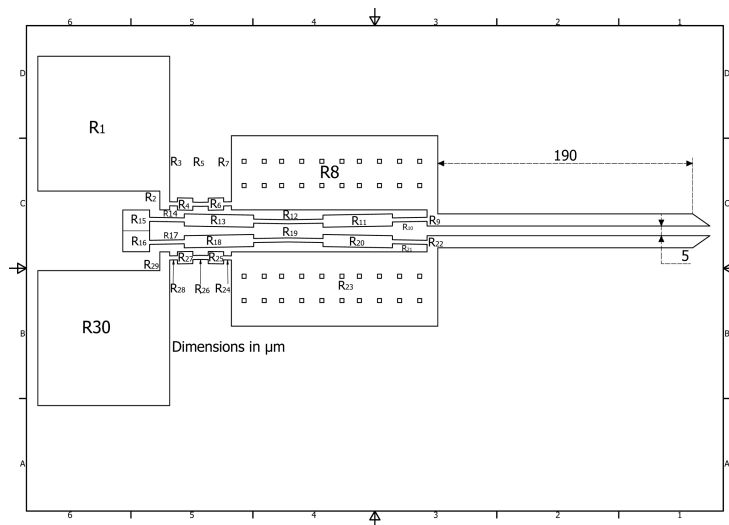


Figure 4. Microgripper based on the modified U-shaped micro-actuator of Figure 2. Dimensions of the jaws are shown.

Next, the mathematical description of the electrical and magnetic properties used in the design of the microgripper is carried out.

The intensity of the electrical current  $I$  can be calculated by using the Equation [32]:

$$I = \frac{V}{R} \quad (1)$$

where  $V$  is the voltage supplied to the device and  $R$  is the resistance that the material opposes to electrical current flow.

The electrical resistance ( $R$ ) of a resistor can be determined from the physical dimensions of each device, such as length and area as well as by its inherent electrical properties of the material with which it was manufactured as the electrical resistivity according to the Equation [32]:

$$R = \frac{\rho l}{A} \quad (2)$$

where  $\rho$  is resistivity,  $l$  is the length and  $A$  is the cross-section area, respectively (Ohm law).

The total resistance of each device is calculated in accordance to the number of sections and configuration,

The corresponding electric power can be calculated by Equation (2).

$$P = VI \quad (3)$$

The increment in temperature, caused by the voltage supply, generates an increment in the body's dimensions. This property is known as thermal deformation and it is mathematically expressed as:

$$\varepsilon = \alpha \Delta T \quad (4)$$

where  $\alpha$  is the thermal expansion coefficient of the corresponding material and  $\Delta T$  denotes the temperature change. Room temperature in this paper was considered as 26.85 °C.

The operation frequency was obtained and adapted from [33] by the mathematical formula

$$f = \frac{1}{2\pi} \sqrt{\frac{Etw^3}{ml^3}} \quad (5)$$

where  $E$  is the Young's modulus of material,  $m$  is the mass of the system,  $t$ ,  $w$  and  $l$  are the thickness, width, and length of the device, respectively.

The stiffness can be calculated using the mathematical expression [34]:

$$k = \frac{F}{\Delta Y_{max}} \quad (6)$$

where  $F$  is the force applied by the tips of the gripper and  $\Delta Y_{max}$  represents their maximum deformation.

The mobility of the modified U-shape micro-actuator is calculated using the well-known Gruebler Equation [35]:

$$DOF = 3L - 2J - 3G \quad (7)$$

Where  $L$  is the number of links,  $J$  is the number of full joints and  $G$  is the number of grounded links.

In the design of the proposed electromechanical microgripper, several physical properties of the material with which its manufacture is planned should be considered. A summary of the mechanical, electrical and thermal properties involved in the microgripper design is found in Table 2.

**Table 2.** Electrical, thermal and mechanical properties of the structural materials used in microgrippers.

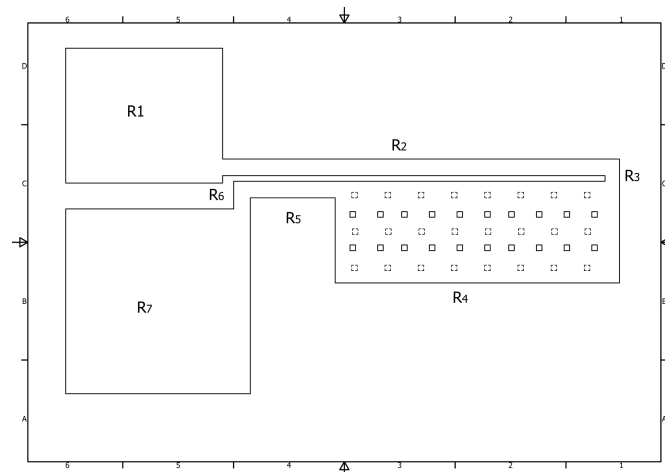
Parameters	Polysilicon [36,37]
Density, $\rho$ [kg/m <sup>3</sup> ]	2230
Young’s Modulus, $E$ [GPa]	158
Thermal expansion coefficient, $\alpha$ [1/°C]	2.8E-6
Isotropic thermal conductivity, $k$ [W/m °C]	32
Poisson Ratio, $\nu$ [Dimensionless]	0.22
Specific Heat, $C_p$ [J/kg °C]	712
Electrical Resistivity, $\rho$ [ $\Omega$ m]	3.3E-5
Melting point, [°C]	1411.85
Tensile Yield strength [GPa]	1.2

### 3. Results

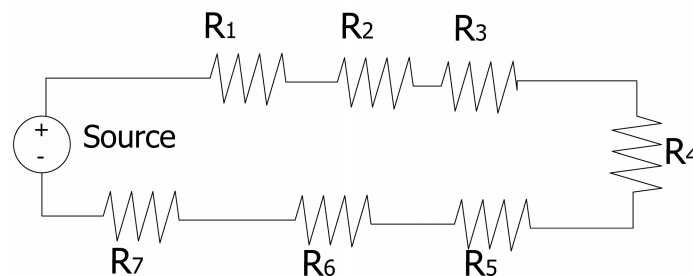
#### 3.1. Results for Initial U-Shaped Actuator

The total electrical resistance  $R_T$  is determined as the equivalent resistance of the series connection of the resistors  $R_1$  to  $R_7$ , which corresponds to each part of it (Figure 5).  $R_T$  is calculated as:

$$R_T = R_1 + R_2 + \dots + R_7 \tag{8}$$



(a)



(b)

**Figure 5.** Initial U-shaped actuator: (a) Isometric scheme and (b) Resistive model.

Performance parameters of the initial U-shaped micro-actuator, obtained by simulation, are shown in Figure 6. A simple approach to characterizing the driving force, and displacement, of Polysilicon U-shaped micro-actuator is provided in [38].

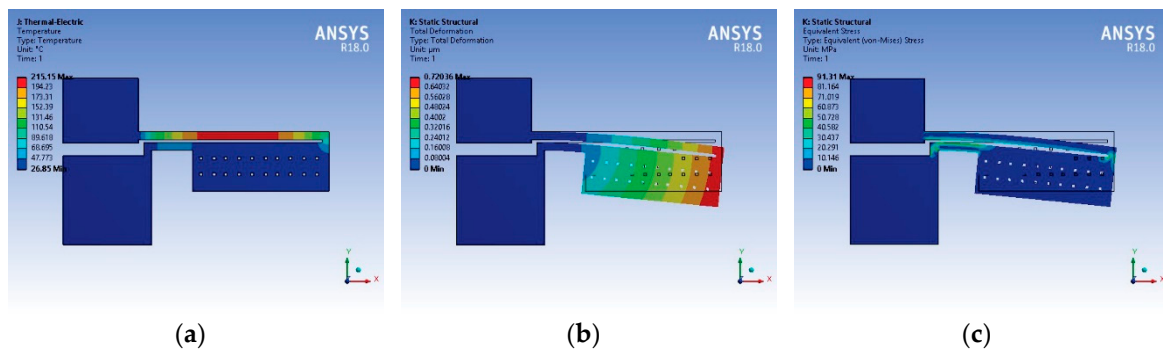


**Figure 6.** Performance parameters of the Polysilicon U-shaped micro-actuator: (a) temperature distribution (b) total deformation, and (c) normal stress.

3.2. Results for Modified U-Shaped Actuator

The isometric scheme and resistive electrical model of U-shaped modified actuator is illustrated in Figure 7.  $R_T$  in this case is determined as the equivalent resistance of the series connection of the resistors  $R_1$  to  $R_{15}$ .

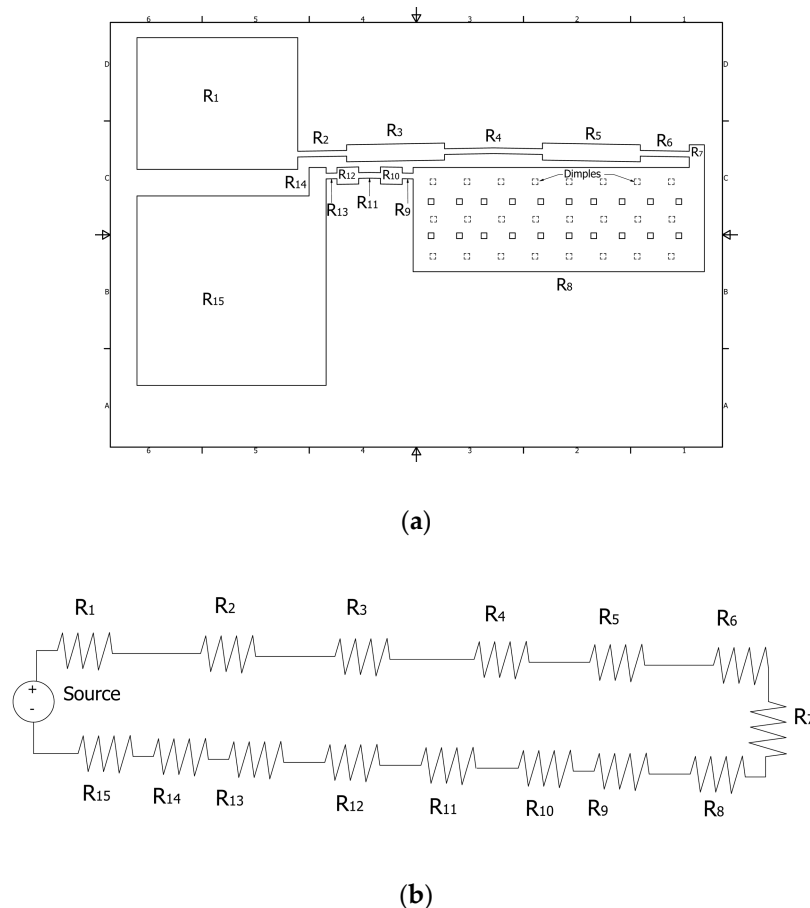


**Figure 7.** Modified U-shaped micro-actuator: (a) Isometric scheme and (b) resistive model.

The mobility of U-shaped micro-actuator is calculated using Equation (7) using the 2G, 5L and 4J (as they can be observed in Figure 8), given only one DOF.

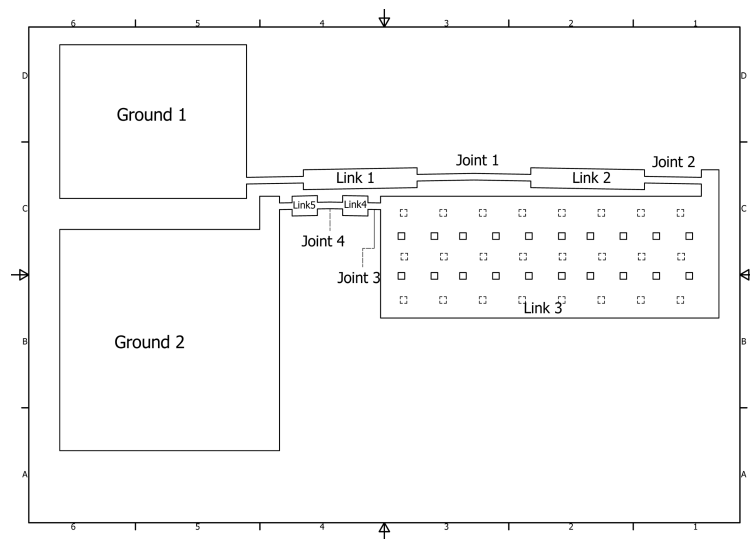


Figure 8. Modified U-shape with Grounds, Links and Joints.

The corresponding performance parameters are shown in Figure 9.

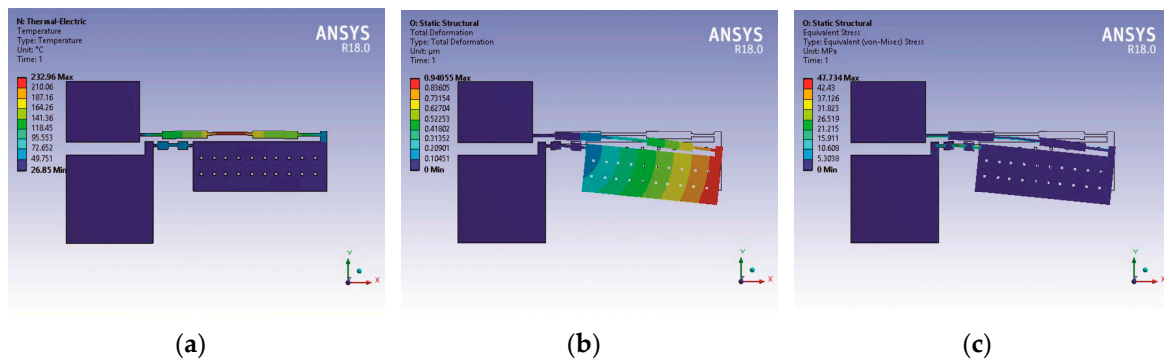


Figure 9. Performance parameters of the Polysilicon modified U-shaped micro-actuator: (a) temperature distribution (b) total deformation, and (c) normal stress.

### 3.3. Results for Microgripper with Modified U-Shaped Micro-Actuator

The calculation for the case of microgripper based on initial U-shaped actuator is not presented, due to its similarity with the modified case here presented. These results are given in Tables 6 and 7.

For Microgripper with Modified U-shaped Micro-actuator, the total electrical resistance is calculated as the parallel between the equivalent resistances of each U-shaped actuator [39], as shown in Figure 10, and in Equation (9), where it is considered that both sides are equal.

$$R_T = \frac{R_{T1}R_{T2}}{R_{T1} + R_{T2}} = \frac{R_{T1}}{2}. \tag{9}$$

with  $R_{T1} = R_1 + R_2 + \dots + R_{15} = R_{T2}$ .

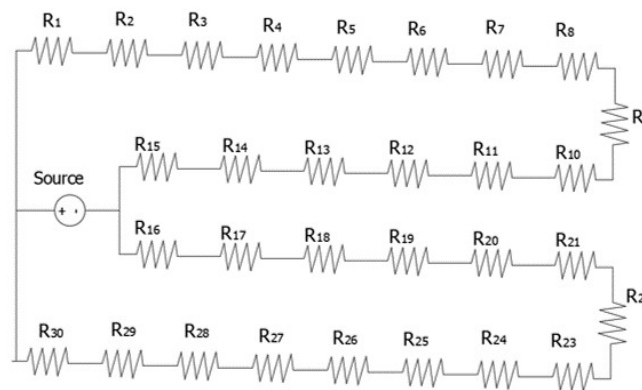


Figure 10. Electrical resistance model for the microgripper based on modified U-shaped micro-actuator.

Performance parameters of the microgripper based on modified U-shaped micro-actuator (total deformation, temperature distribution and normal stress) were obtained by simulation (Figure 11).

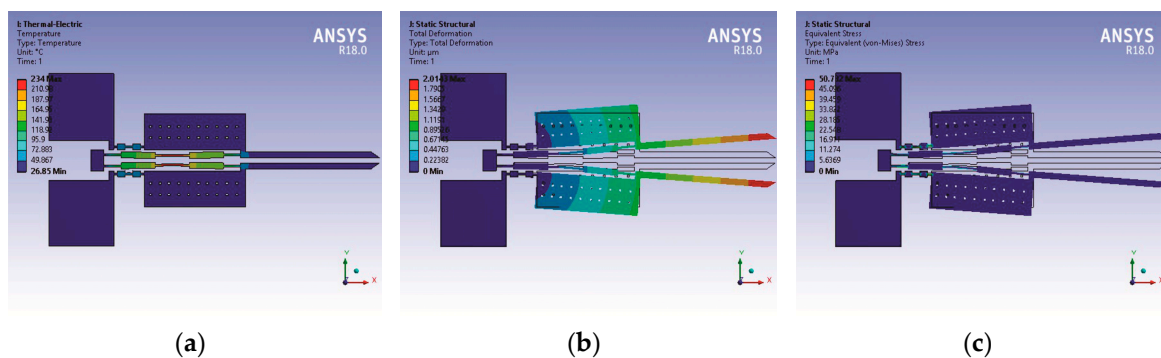


Figure 11. Performance parameters of the Polysilicon microgripper based on Modified U-shaped micro-actuator: (a) temperature distribution, (b) total deformation, and (c) normal stress.

#### 4. Discussion

Simulation results for U-shaped actuators and microgrippers were obtained with the following models with ANSYS Workbench: thermal electric, static structural, and modal module. About the mesh characteristics, some differences were considered (see Table 3).

Table 3. Considerations of mesh in ANSYS Workbench.

Microgripper	Mesh	Elements	Physics Preference
With initial U-shaped actuator	Refinement with relevance = 100	61212	Mechanical
With modified U-shaped actuator	Refinement with relevance = 100	27436	Mechanical

Three conditions were considered:

1. Anchors are fixed
2. Room temperature applied to the wide beam and dimples (300 °K)
3. Convective heat flux (20000 W/m<sup>2</sup> °K)

Thermal convection is one of the three mechanisms of heat transfer, besides conduction and thermal radiation. The heat is transferred by a moving fluid (e.g., wind or water), and is usually the dominant form of heat transfer in liquids and gases. Convection can be divided into natural convection and forced convection [40]. Condition number 3, which was considered the rule of thumb, establishes

that for dimensions less than 1 mm, there will likely not be any free convective currents [41]. If the surrounding fluid is a liquid, then the range of the forced heat transfer coefficients are much wider. For free convection in a liquid  $h \approx 50 - 1,000 \frac{W}{m^2 \cdot K}$  is the typical range. For forced convection, the range is even wider  $h \approx 50 - 20,000 W/m^2 \cdot K$ . In this case, air was considered as the fluid.

In Table 4, total resistance values of the initial and modified U-shaped actuators are given. The values of performance parameters are presented in Table 5.

**Table 4.** Total electrical resistance values of the initial and modified U-shaped micro-actuators.

U-Shaped Structure	Theoretical $R_T$ [ $\Omega$ ]	Simulated $R_T$ [ $\Omega$ ]	% Error
Initial	686.87	691.24	0.63
Modified	1351.35	1299.77	3.96
% Increment	50.82	53.21	

**Table 5.** Values of the performance parameters of U-shaped micro-actuators.

U-Shaped Structure	Total Deformation [ $\mu\text{m}$ ]	Force [ $\mu\text{N}$ ]	Max. Temp. in Thin Arm [ $^\circ\text{C}$ ]	Natural Frequency [MHz]	Electrical Current [mA]	Power [mW]
Initial	0.72036	996.05	215.15	275.65	4.34	13.02
Modified	0.90455	300.08	232.96	261.36	2.3081	6.92
% Increment	25	-230.12	8.27	-5.184	-88.69	-88.15

Note: Negative increment is interpreted as a decrease.

In relation to normal stress of initial and modified U-shaped micro-actuators, they can be observed in the corresponding graphs (6c and 9c, respectively). The largest values correspond to all thinnest segments in thin arms and flexures; these values are 91.34 MPa and 47.734 MPa, respectively. The modified U-shaped micro-actuator shows a decrease of 52.25%. Both values are much smaller than the value of the tensile yield strength for Silicon.

Total resistances for initial and modified microgrippers are given in Table 6.

**Table 6.** Total resistance values of the microgrippers based on initial and modified micro-actuators.

Microgripper	Theoretical $R_T$ [ $\Omega$ ]	Simulated $R_T$ [ $\Omega$ ]	% Error
With initial U-shaped micro-actuator	343.44	345.19	0.5
With Modified U-shaped micro-actuator	675.675	649.51	4
% Increase	50.82	53.14	

Table 7 summarizes the values of the performance parameters of the microgrippers under analysis. It is important to point out that only small differences were obtained between the initial model presented here, and those reported values in [2], but this comparison was not added.

**Table 7.** Values of the performance parameters of microgripper based on initial and modified U-shaped micro-actuator.

Microgripper	Total Deformation [ $\mu\text{m}$ ]	Force [mN]	Max. Temp. in Thin Arm [ $^\circ\text{C}$ ]	Natural Frequency [KHz]	Electrical Current [mA]	Power [mW]
With Initial U-shaped actuator	1.6466	1.825	211.19	16.7	8.691	26.07
With Modified U-shaped actuator	2.0143	0.567	234	12.323	4.619	13.85
% Increment	22.33	-321.86	10.8	-26.2	-53.146	-53.126

Note: Negative increment is interpreted as a decrease.

The equivalent stress values for initial and modified microgrippers was 101.6 MPa and 50.732 MPa, respectively, and this was obtained in the same thinnest parts of the hot arms and flexures in the corresponding U-shaped micro-actuators. Again, this stress has a lower value for the case of the modified microgripper in 49.93%.

From Table 4, it is established that for the case of the U-shaped actuators (initial and modified), the theoretical and simulated values of total resistance are close, since the largest error is 4%. The total resistance of the modified structure is approximately two times, when it is compared with those of the initial structure. In the case of microgrippers based on initial and modified U-shaped micro-actuators, the performance is similar, as it can be seen in Table 6.

For the case of the performance parameters of the U-shaped actuators, shown in Table 5, it can be observed that the improvements obtained with modified thin beam and flexure, reside in a displacement increment of 25%, with an increment in temperature at the middle part of the modified part of the thin beam of 8.27%. Equivalent stress, current and force have lower values. From Table 7, it is possible to deduce that for the case of the microgrippers based on these actuators, they have a similar response. The modified microgripper shows a displacement increment of 22.33%, and an increment in temperature of 10.8% at the middle part of the modified thin beam. Force, current and stress also show notable decrements.

A graphical representation of the performance parameters corresponding to the initial and modified U-shaped micro-actuators and the microgrippers based on them, respectively, was obtained by means of parametric simulation, as shown in Figure 12. It can be observed that there are similar tendencies between the response of the corresponding initial and modified structures, but the values for the cases of force, current, power and total stress are relatively far.

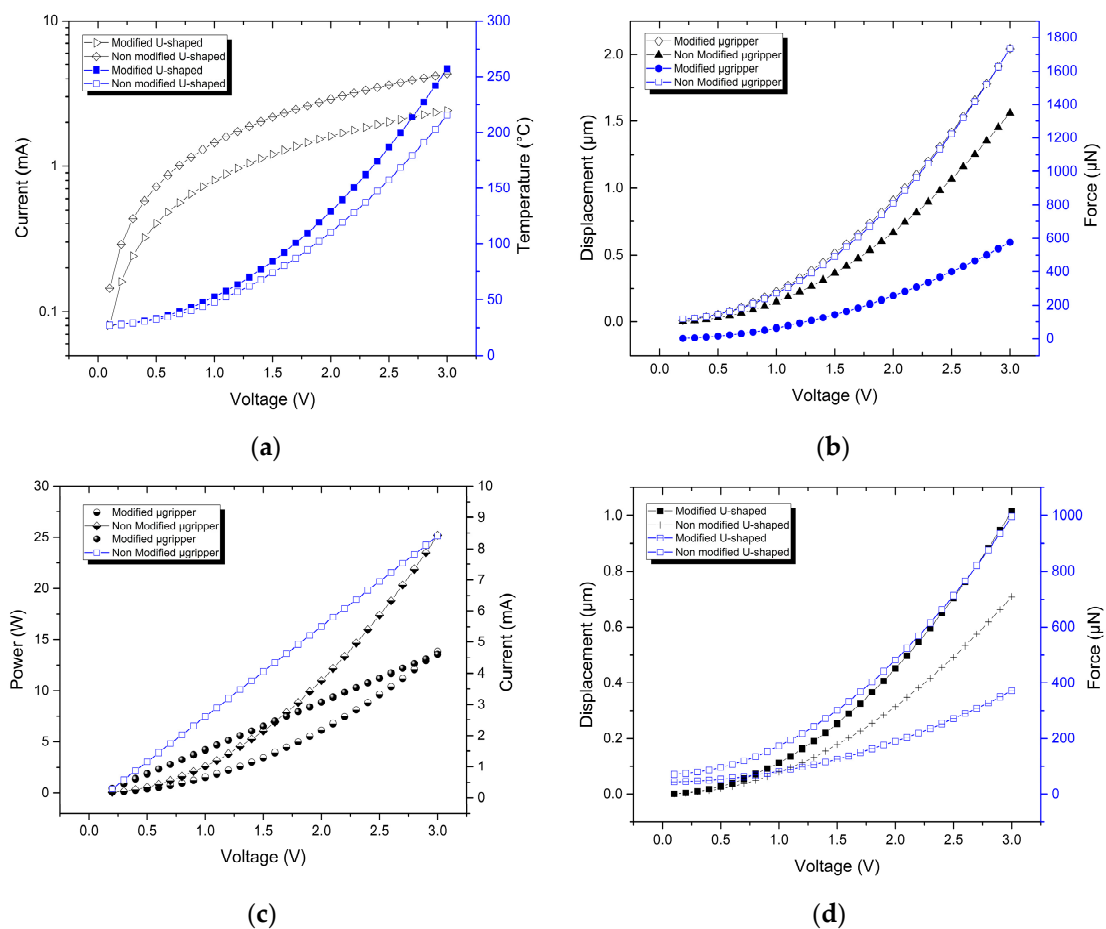
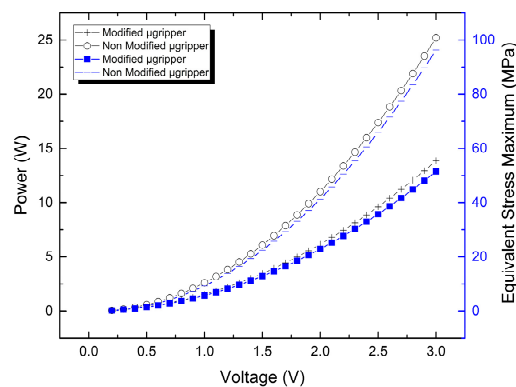


Figure 12. Cont.



(e)

**Figure 12.** For U-shaped micro-actuators: (a) current and temperature distribution versus applied voltage, (b) displacement and force versus applied voltage. For microgrippers: (c) current and power versus applied voltage, (d) displacement and force versus applied voltage; and (e) equivalent stress versus applied voltage.

## 5. Conclusions

In this paper, a new topology of a U-shaped micro-actuator has been presented on the base of lumped compliant mechanisms, designed by means of a mass distribution applied to thin beam and flexure. Fundamental changes in performance parameters are given on displacement, where an increase of 25% is given, but with a notable decrease in force. A reduction in normal stress of 52.25% is also shown. An analogous response is observed for the case of the microgripper based on this modified actuator. In this case, an increase of 22.33% is obtained, but current, power and stress decrease. Force has also the most notable decrement.

The performance parameters considered as fundamental in the electrothermal performance analysis of the microgripper were displacement, force and normal stress (Equivalent Stress Von-Misses). They were obtained by simulation. In addition, current, power and temperature were also analyzed.

The total resistance values obtained from theoretical calculations and simulation were close, since the maximum difference was 4%. Theoretical values of resistance were used for the calculation of current and power, showing good agreement with the corresponding values obtained by simulation.

For the modified microgripper, the reduction in current and power values favors applications which require low values of these parameters. Its lower clamping force facilitates its use when sensitive objects need to be manipulated.

**Author Contributions:** P.V.-C.: Simulation, validation, collaboration and microgripper design. M.T.-T.: Conceptualization of research, collaboration in microgripper design, formal analysis, supervision and editing. R.C.-R.: Resources, methodology and formal analysis. J.A.R.-R.: Supervision. R.V.-B.: Research, writing review and editing.

**Funding:** This research was funded by CONACyT, grant number “A1-S-33433”.

**Acknowledgments:** Pedro Vargas-Chable expresses his sincere gratitude to CONACyT for the scholarships with grant reference 484392.

**Conflicts of Interest:** The authors declare no conflict of interest.

## References

1. Leondes, C.T. *MEMS/NEMS Handbook: Techniques and Applications*; Springer: New York, NY, USA, 2006; Volume 4, ISBN 978-0-387-25786-2.
2. Cauchi, M.; Grech, I.; Mallia, B.; Mollicone, P.; Sammut, N. Analytical, Numerical and Experimental Study of a Horizontal Electrothermal MEMS Microgripper for the Deformability Characterisation of Human Red Blood Cells. *Micromachines* **2018**, *9*, 108. [[CrossRef](#)]

3. Kaźmierski, T.J.; Beeby, S. *Energy Harvesting Systems: Principles, Modeling and Applications*; Springer: New York, NY, USA, 2011; ISBN 978-1-4419-7566-9.
4. Chronis, N.; Lee, L.P. Electrothermally Activated SU-8 Microgripper for Single Cell Manipulation in Solution. *J. Microelectromech. Syst.* **2005**, *14*, 857–863. [[CrossRef](#)]
5. Solano, B.; Wood, D. Design and Testing of a Polymeric Microgripper for Cell Manipulation. *Microelectron. Eng.* **2007**, *84*, 1219–1222. [[CrossRef](#)]
6. Yang, S.; Xu, Q. A Review on Actuation and Sensing Techniques for MEMS-based Microgrippers. *J. Micro-Bio Robot.* **2017**, *3*, 1–14. [[CrossRef](#)]
7. Jia, Y.; Jia, M.; Xu, Q. A Dual-Axis Electrostatically Driven MEMS Microgripper. *Int. J. Adv. Robot. Syst.* **2014**, *11*, 187. [[CrossRef](#)]
8. Kuo, J.-C.; Huang, H.-W.; Tung, S.-W.; Yang, Y.-J. A Hydrogel-based Intravascular Microgripper Manipulated using Magnetic Fields. *Sens. Actuator A-Phys.* **2014**, *211*, 121–130. [[CrossRef](#)]
9. Breger, J.C.; Yoon, C.; Xiao, R.; Kwag, H.R.; Wang, M.O.; Fisher, J.P.; Nguyen, T.D.; Gracias, D.H. Self-Folding Thermo-Magnetically Responsive Soft Microgrippers. *ACS Appl. Mater. Interfaces* **2015**, *7*, 3398–3405. [[CrossRef](#)] [[PubMed](#)]
10. Piriyanont, B.; Moheimani, S.O.R. MEMS Rotary Microgripper with Integrated Electrothermal Force Sensor. *J. Microelectromech. Syst.* **2014**, *23*, 1249–1251. [[CrossRef](#)]
11. Daunton, R.; Gallant, A.; Wood, D.; Katakay, R. A Thermally Actuated Microgripper as an Electrochemical Sensor with the Ability to Manipulate Single Cells. *Chem. Commun.* **2011**, *47*, 6446–6448. [[CrossRef](#)] [[PubMed](#)]
12. Shi, H.; Shi, W.; Zhang, R.; Zhai, J.; Chu, J.; Dong, S. A Micromachined Piezoelectric Microgripper for Manipulation of Micro/Nanomaterials. *Rev. Sci. Instrum.* **2007**, *88*, 065002. [[CrossRef](#)]
13. Jia, Y.; Xu, Q. MEMS Microgripper Actuators and Sensors: The State-of-the-Art Survey. *Recent Pat. Mech. Eng.* **2013**, *6*, 132–142. [[CrossRef](#)]
14. Chen, B.K.; Zhang, Y.; Perovic, D.D.; Sun, Y. MEMS Microgrippers with Thin Gripping Tips. *J. Micromech. Microeng.* **2011**, *21*, 105004. [[CrossRef](#)]
15. Park, D.S.-W.; Nallani, A.K.; Cha, D.; Lee, G.-S.; Kim, M.J.; Skidmore, G.; Lee, J.-B.; Lee, J.-S. A Sub-Micron Metallic Electrothermal Gripper. *Microsyst. Technol.* **2010**, *16*, 367–373. [[CrossRef](#)]
16. Pranonsatit, S.; Holmes, A.S.; Robertson, I.D.; Lucyszyn, S. Single-Pole Eight-Throw RF MEMS Rotary Switch. *J. Microelectromech. Syst.* **2006**, *15*, 1735–1744. [[CrossRef](#)]
17. Iamoni, S.; Soma, A. *Design of an Electro-Thermally Actuated Cell Microgripper*; Springer: Berlin/Heidelberg, Germany, 2014.
18. Chu, J.; Zhang, R.; Chen, Z. A Novel SU-8 Electrothermal Microgripper based on the Type Synthesis of the Kinematic Chain Method and the Stiffness Matrix Method. *J. Micromech. Microeng.* **2011**, *21*, 1–15. [[CrossRef](#)]
19. Seidemann, V.; Büttefisch, S.; Büttgenbach, S. Fabrication and Investigation of In-Plane Compliant SU8 Structures for MEMS and Their Application to Micro Valves and Micro Grippers. *Sens. Actuators* **2002**, *97–98*, 457–461. [[CrossRef](#)]
20. Tsai, Y.C.; Lei, S.H.; Sudin, H. Design and Analysis of Planar Compliant Microgripper based on Kinematic Approach. *J. Micromech. Microeng.* **2005**, *15*, 143–156. [[CrossRef](#)]
21. Kim, K.; Liu, X.; Zhang, Y.; Sun, Y. Nanonewton Force-Controlled Manipulation of Biological Cells using a Monolithic MEMS Microgripper with Two-Axis Force Feedback. *J. Micromech. Microeng.* **2008**, *18*, 1–8. [[CrossRef](#)]
22. Jia, Y.; Xu, Q. Design of a Monolithic Dual Axis Electrostatic Actuation MEMS Microgripper with Capacitive Position/Force Sensors. In Proceedings of the IEEE International Conference on Nanotechnology, Beijing, China, 5–8 August 2013; pp. 817–820.
23. Mackay, R.E.; Le, H. Development of Micro-Tweezers for Tissue Micro-Manipulation. In Proceedings of the 2008 2nd International Conference on Bioinformatics and Biomedical Engineering, Shanghai, China, 16–18 May 2008; pp. 1551–1555.
24. Feng, Y.Y.; Chen, S.-J.; Hsieh, P.-H. Fabrication of an Electro-Thermal Micro Gripper using Silver-Nickel Ink. In Proceedings of the IEEE 29th International Conference on Micro Electro Mechanical Systems (MEMS), Shanghai, China, 28 July 2016.
25. Bazaz, S.A.; Khan, F.; Shakoor, R.I. Design, Simulation and Testing of Electrostatic SOI MUMPs based Microgripper. *Sens. Actuator A-Phys.* **2011**, *167*, 44–53. [[CrossRef](#)]

26. Shivhare, P.; Uma, G.; Umopathy, M. Design Enhancement of a Chevron Electrothermally Actuated. *Microsyst. Technol.* **2015**, *22*, 2623–2631. [CrossRef]
27. Velosa-Moncada, L.; Aguilera-Cortés, L.A.; González-Palacios, M.; Raskin, J.-P.; Herrera-May, A.L. Design of a Novel MEMS Microgripper with Rotatory Electrostatic Comb-Drive Actuators for Biomedical Applications. *Sensors* **2018**, *18*, 1664. [CrossRef]
28. Fu, Y.; Du, H. Fabrication of micromachined TiNi based microgripper with compliant structure. *Proc. SPIE* **2003**. [CrossRef]
29. Verotti, M.; Dochshanov, A.; Belfiore, N. A Comprehensive Survey on Microgrippers Design: Mechanical Structure. *J. Mech. Des.* **2017**, *139*, 1–26. [CrossRef]
30. Stolarski, T.; Nakasone, Y.; Yoshimoto, S. *Engineering Analysis with ANSYS Software*; Butterworth-Heinemann: Oxford, UK, 2006; ISBN 0-7506-6875-X.
31. Feng, Y.Y.; Chen, S.J.; Hsieh, P.H.; Chu, W.T. Fabrication of an Electro-Thermal Micro-Gripper with Elliptical Cross-Sections using Silver-Nickel Composite Ink. *Sens. Actuator A-Phys.* **2016**, *245*, 106–112. [CrossRef]
32. Askeland, D.R.; Wright, W.J. *The Science and Engineering of Materials*, 7th ed.; Cengage Learning: Boston, MA, USA, 2016; ISBN 978-1-350-07676-1.
33. Cabello-Ruiz, R.; Tecpoyotl-Torres, M.; Torres-Jacome, A.; Grimalsky, V.; Vera-Dimas, J.G.; Vargas-Chable, P. A Novel Deformation-Amplifying Compliant Mechanism Implemented on a Modified Capacitive Accelerometer. *Int. J. Electr. Comput. Eng.* **2017**, *7*, 1858–1866. [CrossRef]
34. Johnstone, R.W.; Parameswaran, M. Modelling Surface-Micromachined Electrothermal Actuators. *Can. J. Elect. Comput. Eng.* **2004**, *29*, 193–202. [CrossRef]
35. Abu-Zarifa, A. Theory of Machines. Islamic University of Gaza. Department of Mechanical Engineering. 2012. Available online: [http://site.iugaza.edu.ps/wp-content/uploads/file/IUGAZA%20TOM2012\\_CH1-2.pdf](http://site.iugaza.edu.ps/wp-content/uploads/file/IUGAZA%20TOM2012_CH1-2.pdf) (accessed on 4 March 2019).
36. Ghodssi, R.; Lin, P. *MEMS Materials and Processes Handbook*; Springer: New York, NY, USA, 2011; ISBN 978-0-387-47318-5.
37. Sharpe, N.J.; Yuan, B.; Vaidyanathan, R.; Edwards, R.L. Measurements of Young's Modulus, Poisson's Ratio, and Tensile Strength of Polysilicon. In Proceedings of the Tenth IEEE International Workshop on Microelectromechanical Systems, Nagoya, Japan, 26–30 January 1997.
38. Huang, Q.A.; Leer, N.K. A simple approach to characterizing the driving force of polysilicon laterally driven thermal microactuators. *Sens. Actuators* **2000**, *80*, 267–272. [CrossRef]
39. Nilsson, J.W.; Riedel, S.A. *Electric Circuits*, 10th ed.; Pearson: Harlow, UK, 2015; ISBN 978-0-13-376003-3.
40. Green TEG AG. Convective Heat Flux Explained. Zürich, Switzerland. Available online: <https://www.greenteg.com/template/userfiles/files/Convective%20Heat%20Flux%20Explained.pdf> (accessed on 18 February 2019).
41. Modeling Natural and Forced Convection in COMSOL Multiphysics®. Available online: <https://www.comsol.com/blogs/modeling-natural-and-forced-convection-in-comsol-multiphysics/> (accessed on 4 March 2019).



© 2019 by the authors. Licensee MDPI, Basel, Switzerland. This article is an open access article distributed under the terms and conditions of the Creative Commons Attribution (CC BY) license (<http://creativecommons.org/licenses/by/4.0/>).